Realization of Closed Cavity Resonator Formed by Graphene-PMMA Membrane for Sensing Audio Frequency

Realization of Closed Cavity Resonator Formed by Graphene-PMMA Membrane for Sensing Audio Frequency

Jing Xu, Graham S. Wood, *Member, IEEE,* Asaad K. Al-mashaal,
Enrico Mastropaolo, Michael J. Newton and Rebecca Cheung, *Senior Member, IEEE*

***Abstract*—Large area graphene-poly (methyl methacrylate) (PMMA) closed cavity resonator has been fabricated. The resonator has been formed by transferring an ultra-large graphene-PMMA membrane over 3.5 mm diameter circular closed cavity with 220 μm depth. The graphene-PMMA membrane includes 6-layer graphene and 450 nm PMMA film. A modified graphene-PMMA dry transfer method has been developed in this work. Using the Kapton tape supporting frame, the graphene-PMMA membrane has been dry transferred onto the substrate with a small membrane's static deformation of around 180 nm. The membrane's static deformation aspect ratio (suspended membrane's diameter over the membrane's deformation) is around 19,500. The graphene-PMMA closed cavity resonator has been actuated mechanically, acoustically and electro-thermally. The dynamic behaviour of the membrane suspended over the closed cavity shows that the (1, 1) mode dominates the graphene-PMMA membrane's resonance with a resonant frequency of around 10 kHz and suggests the device is under good gas encapsulation. Acoustic vibration amplitude sensitivity of graphene-PMMA membrane over the closed cavity is measured to be around 6 μm/Pa. The membrane's dynamic behaviour, simulated under similar mechanical and electro-thermal actuation conditions, has been shown to be consistent with the trend of the device's experimental results. The strain in the suspended graphene-PMMA membrane is estimated to be 0.04 $\pm$ 0.01 %.**

***Index Terms*—graphene, graphene dry transfer, PMMA, Raman, resonant frequency, acoustic resonator, MEMS.**

I. Introduction

MECHANICAL graphene resonators in the micro- and nano- scale have been reported to possess outstanding properties, including ultralow mass, high quality factor and high sensitivity [1]–[7]. The remarkable electrical and mechanical properties of graphene, such as high electron mobility of 200 000 $cm^2V^{-1}s^{-1}$ [8], low mass density of 2200 kg/m^3 [9], and ultra-high Young's modulus of 0.5 to 1 TPa, promise the potential of achieving graphene acoustic devices with high sensitivity. Some graphene-based acoustic sensors with good performance, including microphones, open cavity resonators and loudspeakers, have been fabricated successfully in the past [9]–[15]. Such devices have graphene-based membrane aspect ratios, defined as the diameter to thickness ratio for the membrane, between 3400 and 350,000.

To target the audio frequency range, processes for fabricating large aspect ratio graphene membranes around a few millimetres' diameter are necessary. Unlike the micrometre diameter graphene-based resonators [2]–[7], the millimetre diameter membranes are much more difficult to be suspended or clamped fully over the cavity due to the larger membranes' diameter to thickness aspect ratio. In particular, monolayer and few layer graphene membranes could be damaged easily. Therefore, graphene-based membranes in previously reported acoustic sensors have been thickened by increasing the graphene layer number from 67 [10] to 1800 [12] or by attaching 200 nm to 3 μm thick PMMA layer [12], [13], in order to increase the robustness of the membrane. The advantage of using PMMA as the supporting layer instead of increasing the graphene layer number by 1 to 3 orders of magnitude, is that lower resonant frequency can be achieved from the graphene-PMMA bilayer due to the lower density and elasticity of PMMA.

Previously, the fabrication methods developed for capacitive graphene-based microphones [10]–[13], involve multiple steps, have been assembled manually and may have air leaking into the devices. The reported process is complex and can decrease the consistency of the devices' characteristics as a result of the manual assembling steps. Nevertheless, the devices reported exhibit relatively high sensitivity, ranging from -70 dB V to -20 dB V [10]–[13], [15].

Recently, an ultra-large graphene-PMMA open cavity resonator [9], [14], has been reported by us. However, this design is not suitable for integration into the circuit system because the bottom electrode cannot be processed in the open cavity configuration. In addition, the open cavity device had been made using a wet transfer method. To fabricate large aspect ratio graphene-based membrane onto a closed cavity device, where electrical connections can be integrated into the substrate, it is necessary to use a dry transfer method since in the wet transfer method, liquid could be trapped inside the closed cavity.

J. Xu, G. S. Wood and R. Cheung are with the School of Engineering, Institute for Integrated Micro and Nano Systems, University of Edinburgh, Edinburgh, EH9 3FF, U.K. (e-mail: jing.xu.2@ed.ac.uk; g.s.wood@ed.ac.uk; r.cheung@ed.ac.uk).

A. K. Al-mashaal was with the School of Engineering, Institute for Integrated Micro and Nano Systems, University of Edinburgh, Edinburgh, EH9 3FF, U.K. He is now with the Polymer Research Center, University of Basrah, Basrah 61004, Iraq. (e.mail: asaad.al@ed.ac.uk).

E. Mastropaolo, deceased, was with the School of Engineering, Institute for Integrated Micro and Nano Systems, University of Edinburgh, Edinburgh, EH9 3FF, U.K.

M. J. Newton is with the Acoustics and Audio Group, University of Edinburgh, Edinburgh, EH8 9DF, U.K. (e.mail: michael.newton@ed.ac.uk).

Indeed, there are many challenges associated with suspending graphene-based membrane with large aspect ratio over a closed cavity as a device for acoustic sensing, namely, the optimization of the spacing between the membrane and the substrate, the prevention of the membrane from shorting the device by touching the substrate and the minimization of damping effects within the formed cavity. Thus far, despite the progress made in the fabrication and characterisation of graphene-based acoustic sensors, the resonance and associated dynamic deformation of the graphene-based acoustic sensors have not been studied, which are significant in understanding the membrane's characteristics and hence, improving the performance of the graphene-based acoustic sensors.

In this work, we have developed a simplified one-step reliable process for fabricating a graphene-PMMA closed cavity resonator with an optimum gap of 220 μm for acoustic sensing. The bilayer membrane, with aspect ratio of 7800 over the closed cavity, includes 6-layer graphene and 450 nm PMMA. The device has been formed by a simplified one-step graphene-PMMA dry transfer method using Kapton tape as a supporting frame. Because the graphene-PMMA membrane has been attached and sealed on the closed cavity substrate by van der Waals force, the gas encapsulation is better than the devices in which the membrane and the substrate are connected by case or cartridge via manual assembly. The static deformation of graphene-PMMA membrane suspended over the closed cavity has been measured in this study. Furthermore, the dynamic resonance characteristics of the graphene-PMMA closed cavity resonator actuated mechanically, acoustically and electro-thermally have been determined for the first time.

II. Device design and operating principles

Fig. 1(a) shows the structure of the graphene-PMMA closed cavity resonator which has been fabricated by transferring an ultra large area of graphene-PMMA membrane, over the closed circular cavity with 220 μm depth and 3.5 mm diameter. Fig. 1(b) shows an optical image of the resonator after transferring the graphene-PMMA layer over the closed cavity.

450 nm poly (methyl methacrylate) (PMMA) layer has been spin-coated on the 6 layers graphene as a supporting layer, to improve the stability of the graphene resonator and decrease the resonant frequency of the bilayer membrane. The resonant frequency formula for such a membrane [9] is:

$$t_{\text{eff}} = t_{\text{g}} + t_{\text{p}}, \tag{1}$$

$$\rho_{\text{eff}} = \frac{\rho_{\text{g}} t_{\text{g}} + \rho_{\text{p}} t_{\text{p}}}{t_{\text{g}} + t_{\text{p}}}, \tag{2}$$

$$f_{\text{mn}} = \frac{\beta_{\text{mn}}}{2\pi R} \sqrt{\frac{N}{\rho_{\text{eff}} t_{\text{eff}}}}, \tag{3}$$

where t and ρ are thickness and density of the material, t_{eff} and ρ_{eff} refer to the effective thickness and effective density for graphene (g)/PMMA (p) bi-layer membrane, R is the radius of the membrane, ρ is the density of the material, N is the tension in the membrane and β_{mn} is a dimensionless coefficient of the resonant mode.

The (0,1) and (1,1) modes of resonant frequency in such bilayer membrane has been estimated to be within the audio frequency range (20 Hz to 20 kHz), with the assumption of the 2.0 N/m tension in the membrane [9].

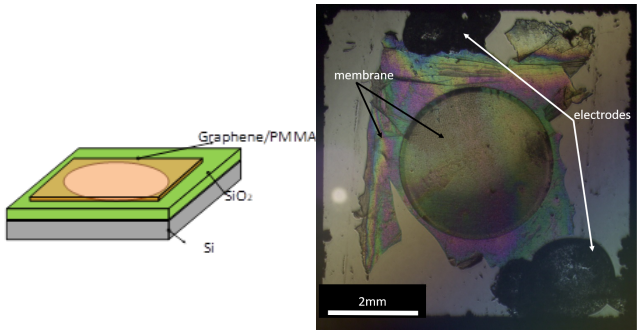

(a) (b)

Fig. 1. The schematic (a) and the optical image (b) of the graphene-PMMA membrane closed cavity resonator with the silver paste as electrodes.

III. Materials and methods

Fig. 2 illustrates the fabrication process of the graphene-PMMA closed cavity resonator, including the hollow substrate fabrication, modified graphene dry transfer method and the optical image of the graphene-PMMA membranes with the Kapton tape frame. Fig. 2(a) displays the procedure of making the hollow substrate. First, 500 nm silicon dioxide has been deposited on the silicon. Next, 3.5 mm diameter hole has been patterned. After the silicon oxide layer on the cavity has been etched by reactive-ion etching (RIE), the silicon inside the cavity has been etched by deep reactive-ion etching (DRIE) to form a well with 220 μm depth.

Fig. 2(b) shows the process of the dry transfer using the Kapton tape as a supporting frame. Firstly, 450 nm PMMA has been spin coated on the chemical vapor deposition (CVD) grown multilayer graphene copper foil. Kapton tape has been used to attach the edges of the PMMA/graphene/copper foil. Next, the copper has been etched away with 4.5% ferric chloride solution. After the membrane has been dried in the air completely, the membrane with Kapton tape frame has been transferred onto the substrate on the hot plate at a temperature of 140°C which is inside the range of PMMA glass-transition temperature (105°C-165°C) [16], [17]. The membrane has been stuck on the substrate immediately when using a brush to make the membrane contact fully onto the substrate. When PMMA is heated to the glass-transition phase, the membrane area expands and the contact area enlarges. As a result, the adhesion between graphene-PMMA and silicon dioxide substrate increases [16], [17]. When the chip has been cooled down to room temperature, the frame could be peeled off easily from the sample once the membrane has been clamped fully on the substrate.

Fig. 2(c) shows the optical image of the graphene-PMMA membrane with the Kapton tape supporting frame. The membrane is observed to be flat and without folding or wrinkling. The residual etchant has been cleaned by the DI water.

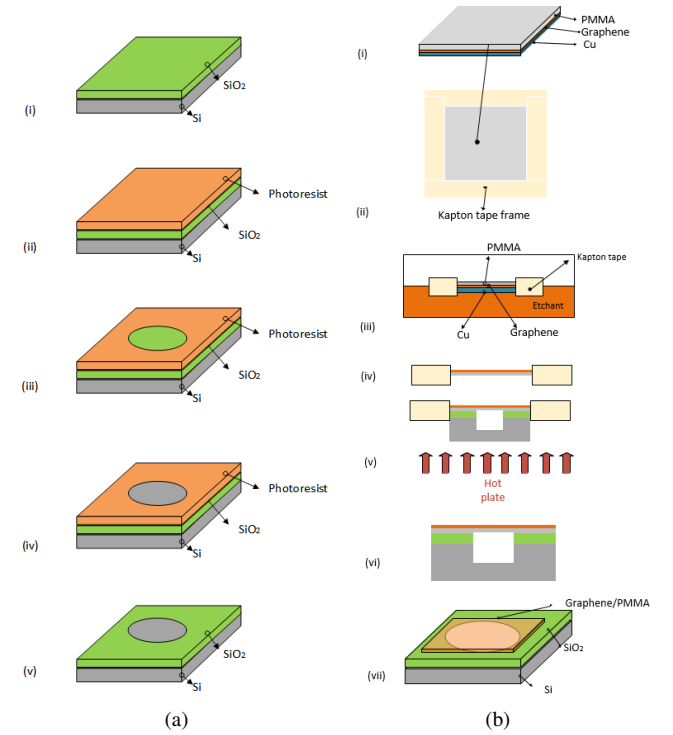

Fig. 2. The fabrication process of the graphene-PMMA closed cavity resonator: (a) fabrication process of the substrate: (i) 500 nm oxide deposited on the silicon with PECVD; (ii) spin coat the 7 μm photoresist; (iii) pattern 3.5 mm diameter holes; (iv) etch silicon dioxide with RIE and silicon with DRIE; (v) dissolve the photoresist with acetone. (b) the modified dry transfer method process: (i) spin coat PMMA on the graphene/copper foil; (ii) use the Kapton tape to make a frame; (iii) wet etch the copper; (iv) dry the membrane in the air; (v) transfer the membrane onto the substrate on the hot plate on the temperature of 140°; (vi) peel off the frame after the substrate cooled down; (vii) the sample schematic illustration. (c) The optical image of graphene-PMMA membrane with Kapton tape supporting frame.

The supporting frame has prevented the wet membrane from touching and sticking on the container surface.

In our work, the modified graphene-PMMA dry transfer method is faster and simplified for suspending ultra-large graphene-based membrane. In previous work, the graphene has been dry transferred to small features around a few microns [16], [17]. The graphene with the Polydimethylsiloxane (PDMS) supporting frame requires more than 12 hours heating [17] or high temperature at around 200°C [16]. Here, for the large feature design, a brush could be used to make contact between the membrane and substrate, which replaces the long time and high temperature heating. In addition, the Kapton tape has been used to attach the edges of the membrane and work as a frame. Unlike PDMS, using Kapton tape frame does not require the step of patterning or etching the polymer, and decreases the process complexity. In previous research, the Kapton tape frame [10] with a hole in the centre has also been used as a supporting frame and spacer and has been included into the devices. Here, the Kapton tape frame can be peeled off easily once the membrane has been stuck on the substrate. This modified dry transfer method for ultra-large graphene-PMMA membrane has been conducted with 95 % success rate over 20 samples.

The graphene-PMMA closed cavity resonator has been characterized by: white light interferometry (WLI, Zygo), Polytec laser Doppler Vibrometer (LDV) and Raman Spectroscopy (inVia Renishaw). The static deformation is measured by WLI. Additionally, the dynamic behaviour actuated mechanically, acoustically and electro-thermally, is detected by the LDV. The presence of graphene is studied by Raman Spectroscopy.

IV. Results and Discussion

A. Static deformation

From the WLI measurements, the graphene-PMMA membrane has been found to deform by around 180 nm after it has been transferred over the closed cavity.

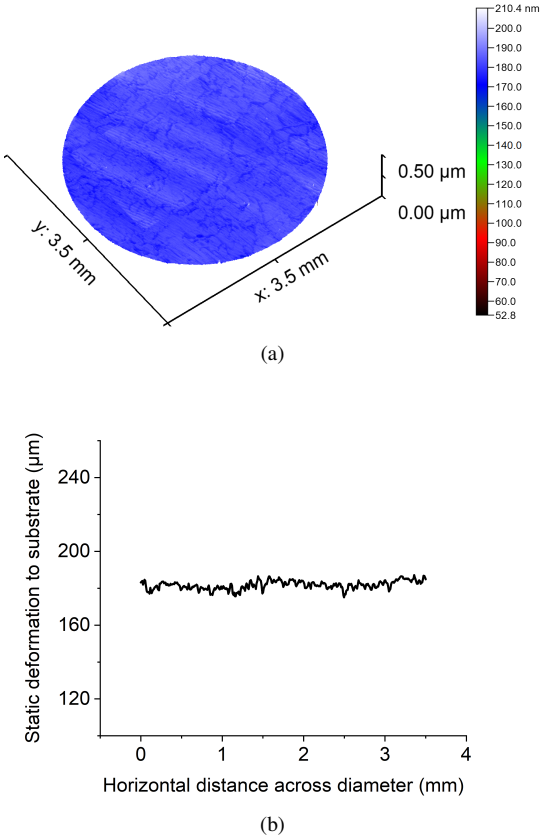

Fig. 3. The static measurement with WLI: (a) the topography and (b) the cross section of the graphene-PMMA membrane over the diameter.

The three-dimensional image of the graphene-PMMA membrane suspended over the substrate is shown in Fig. 3(a).

As the cross section over the membrane's diameter has been illustrated in Fig. 3(b), the static deformation of the membrane has been measured to be around 180 nm. The membrane's static deformation aspect ratio (the membrane's diameter over the membrane's static deformation) is about 19,500. The static measurement indicates the surface static deformation is extremely small when using the Kapton tape frame dry transfer method to transfer ultra-large graphene-PMMA membrane over the closed cavity resonator.

B. Dynamic actuation

The dynamic behaviour has been performed by actuating the graphene-PMMA membrane over the closed cavity by a sweep of sine wave, mechanically, acoustically, and electro-thermally. For the mechanical actuation: the graphene-PMMA closed cavity resonator has been placed on the piezoelectric disk. The disk has been actuated by a sweep of AC voltage from 0.1 V to 2 V. For acoustic actuation: a speaker has been placed next to the graphene-PMMA closed cavity resonator. The sound pressure (sound volume) has been changed from 0.002 Pa (40 dB) to 0.04 Pa (66 dB). For the electro-thermal actuation: silver paste has been attached on the two sides of the membrane edge, serving as two electrodes. The input voltage to electrodes connected to the membrane is held constant at 1 V DC while AC voltage is varied from 1 V to 9 V. Using different actuation methods, the resonant frequency of the graphene-PMMA membrane over closed cavity is detected to be around 10.58 kHz $\pm 10\%$, which is within the audio frequency range. The membrane is measured to exhibit the (1, 1) mode at the resonant frequency.

1) Mechanical actuation: The frequency response of the graphene-PMMA membrane actuated mechanically is shown in Fig. 4(a). As the input AC voltage to the piezo-electric disk increases from 0.1 V to 2 V, the displacement amplitude of the graphene-PMMA membrane over the closed cavity at 11.72 kHz has been observed to rise from 12.6 nm to 237.3 nm. Around the membrane′s resonant frequency at 11.72 kHz, other peaks, at about 6 kHz and 8 kHz are observed. This is probably due to the noise caused by the piezo-disk since the peaks at the frequencies around 6 kHz and 8 kHz disappear when the membrane is actuated acoustically and electro-thermally, as shown in Fig. 4(b) and Fig. 4(c). The results from the mechanical actuation illustrate that the graphene-PMMA membrane over closed cavity is changing by varying the mechanical pressure.

2) Acoustic actuation: The graphene-PMMA membrane's frequency response, to increasing sound pressure from 0.002 Pa (40 dB) to 0.04 Pa (66 dB) has been measured. Fig. 4(b) shows that the resonant displacement of the membrane increases with the sound pressure. The displacement rises from 13.3 nm to 246.8 nm with increase of the sound pressure. 10.58 kHz is the resonant frequency observed for the graphene-PMMA membrane over closed cavity by acoustic actuation. The acoustic actuation measurement shows that the graphene-PMMA membrane over the suspended cavity is sensitive to sound pressure.

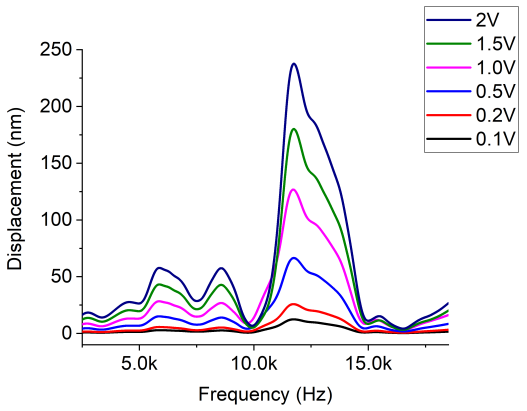

(a)

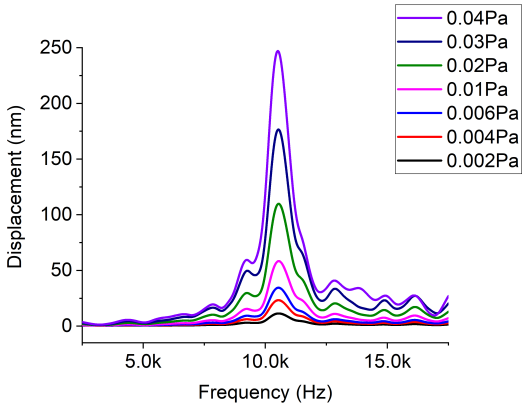

(b)

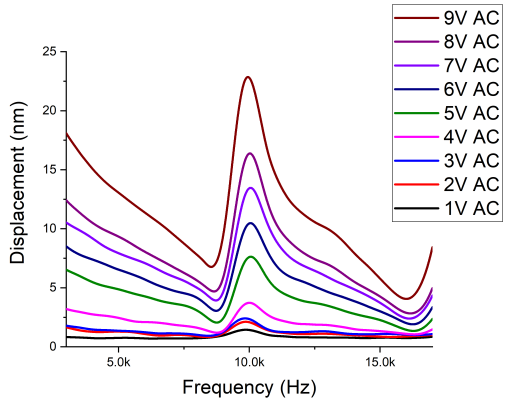

(c)

Fig. 4. The frequency response measured at (a) mechanical actuation with input AC voltage from 0.1 V to 2 V; (b) acoustic actuation with sound pressure from 0.002 Pa to 0.04 Pa; (c) electro-thermal actuation with AC input voltage from 1 V to 9 V and constant 1 V DC voltage.

3) Electro-thermal actuation: The electro-thermal actuation experiment is conducted by keeping constant 1 V DC voltage and changing AC voltage from 1 V to 9 V. As shown in Fig. 4(c), the displacement of membrane increases from 1.4 nm to 21.6 nm with increasing AC input. The resonant frequency is detected to be around 10 kHz.

From the frequency response measurement, the quality factor of the membrane has been estimated to be 6.63 $\pm 0.05\%$, 13.78 $\pm 0.01\%$ and 7.51 $\pm 0.05\%$ under mechanical, acoustic and electro-thermal actuation respectively.

C. Sensitivity of vibration amplitude

The sensitivity of the vibration amplitude has been calculated by fitting the resonant displacement of the membrane versus the input signal. As shown in Fig. 5, the black squares represent the experimental results and the red dash lines correspond to the fitting. In the case of mechanical and acoustical actuation, the vibration amplitude has been observed to be linear with the input signal. For the electro-thermal actuation, the vibration amplitude shows a quadratic relation with the input AC voltage.

In the case of electro-thermal actuation, the current goes through the membrane and generates heating in the graphene-PMMA membrane. The vibration of the membrane is introduced by thermal stress due to Joule Heating. The displacement is proportional to the thermal stress and therefore can be derived in the quadratic relationship with input voltage [18], [19]. The relationship between the thermal stress and input voltage has been confirmed by simulations (see section E).

As shown in Table I, the vibration amplitude sensitivity of the graphene-PMMA membrane over the closed cavity is calculated to be around 120 nm/V by mechanical actuation, 6 μm/Pa by acoustic actuation and 0.3 nm/V^2 by electro-thermal actuation.

The membrane's high sensitivity by acoustic actuation indicates the potential of applying graphene-PMMA membrane over the closed cavity resonator to high sensitivity condenser microphone and loudspeaker.

D. Mode shape

Fig. 6 shows the graphene-PMMA membrane mode shapes at the resonant frequency under the three different types of actuation methods. Fig. 6(a) to c illustrate the mode shapes of the same membrane suspended over the closed cavity under the mechanical (0.1 V AC), acoustic (0.002 Pa/40 dB) and electro-thermal (1 V AC and 1 V DC) actuation respectively. From the mode shapes shown in Fig. 6, it can be seen that the (1, 1) mode of the graphene-PMMA membrane has been actuated and dominates the frequency response in the closed cavity. Unlike the open cavity device, where the (0, 1) mode resonance dominates [9], and the air could flow freely through the open hole, in the case of graphene-PMMA closed cavity resonator, the impermeability of the graphene layer [20] and the closed cavity substrate seal the air inside the closed cavity. The change of gas volume inside the closed cavity is too small to support the relatively large membrane movement needed to generate the large volume change in the (0, 1) resonant mode. Therefore, in the graphene-PMMA closed cavity resonator where gas encapsulation is good, and hence only small gas volume changes, the observed (1, 1) mode resonance is dominant.

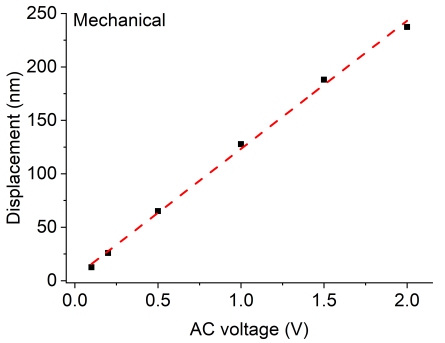

(a)

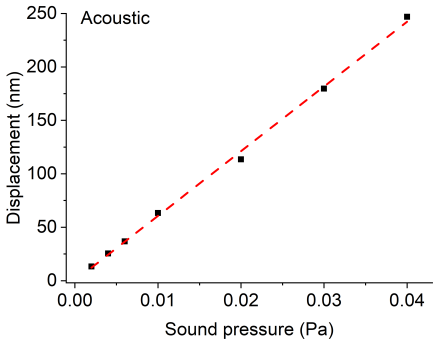

(b)

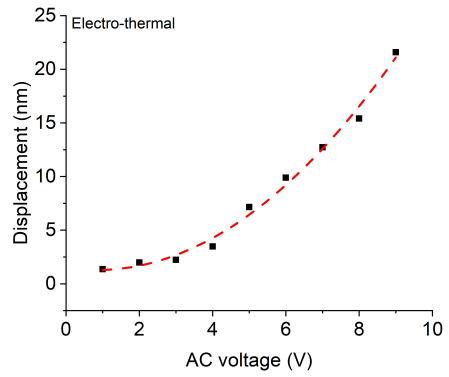

(c)

Fig. 5. The resonant displacement vibration amplitude sensitivity versus (a) mechanical actuation with input AC voltage from 0.1 V to 2 V; (b) acoustic actuation with sound pressure from 0.002 Pa to 0.04 Pa; (c) electro-thermal actuation with AC input voltage from 1 V to 9 V and constant 1 V DC voltage.

In addition, the orientation of the mode shape has been observed to change depending on the actuation methods. For mechanical actuation, the orientation has been observed to be determined by the position of the piezo-disk; for the acoustic actuation, the orientation has been detected to vary with the position of the speaker and for the electro-thermal actuation, the mode shape orientation changes with the position of the electrodes.

In order to achieve the resonance of the ultra-large graphene-PMMA membrane suspended over the closed cavity, an optimized air gap distance of 220 μm has been found. In the

TABLE I
SENSITIVITY OF VIBRATION AMPLITUDE

Actuation methods	*Varying input signal range*	*Measured resonant frequency*	*Sensitivity of vibration amplitude*
Mechanical	0.1 V to 2 V AC	11.72 kHz	119.74 nm/V
Acoustic	0.0002 Pa to 0.04 Pa	10.58 kHz	6.06 μm/Pa
Electro-thermal	1V to 9 V AC	10.01 kHz	0.3 nm/V^2

investigation of the relationship between the air gap distance and the dynamic behaviour of the membrane over the closed cavity, the resonance for the acoustic frequency range of the graphene-PMMA membrane over the closed cavity could not be observed when the air gap distance has been decreased. The disappearance of the resonance in the closed cavity device with smaller air gap distance might be due to damping effects [16], [20]. Our observation suggests that in the previously reported graphene-based microphone designs [10]–[13], [15], there might be the presence of air leaking in the connection between devices' substrates and the graphene-based membranes attached on the supporting frames.

E. Simulations

Finite element analysis (FEA) simulations of the device under mechanical and electro-thermal actuation have been performed with Coventorware 10, in order to investigate the relationship between the actuation stress and the input signal. To simulate mechanical actuation, pressure from 0.01 Pa to 0.1 Pa has been applied on the bottom surface of the silicon substrate. As shown in Fig. 7(a), the stress and displacement of the graphene-PMMA membrane a linear relationship with the input pressure and is consistent with the measured results. In the case of electro-thermal actuation, voltages from 1 V to 10 V have been applied to the electrodes. As Fig. 7(b) illustrates, the thermal actuation stress over the membrane has a quadratic relationship with the input voltage for electro-thermal actuation. The temperature increase as a function of input voltage has also been plotted. As the displacement is proportional to the thermal stress, the simulations confirm the experimental results. Fig. 7(c) shows that the graphene-PMMA membrane suspended over the closed cavity has been observed to be under (1, 1) mode for both the mechanical and electro-thermal actuation.

F. Strain analysis

In addition to the actuation stress derived from simulations, the strain, including built-in strain and actuation strain, in the graphene-PMMA membrane over the closed cavity has been estimated from both the experimentally measured resonant frequency and Raman shift.

1) The strain can be deduced from the measured resonant frequency using:

$$A_{\mathrm{m}} = \frac{\rho_{\mathrm{air}} R}{3\rho_{\mathrm{eff}} t_{\mathrm{eff}}}, \tag{4}$$

$$f_{\mathrm{mn}} = \frac{\beta_{\mathrm{mn}}}{2\pi R}\sqrt{\frac{N_{\mathrm{i}} + N_{\mathrm{a}}}{\rho_{\mathrm{eff}} t_{\mathrm{eff}}(1 + A_{\mathrm{m}})}}, \tag{5}$$

where ρ_{air} is the air density, A_{m} is the air mass, N_{i} and N_{a} represent the built-in tension and the tension caused by the dynamic actuation.

The tension and strain of the graphene-PMMA membrane have been calculated with equation (5) [9]. The air mass is considered, since the resonance measurement of the sample has been conducted in air medium [21]. As shown in Table II, the tension ($N_{\mathrm{i}} + N_{\mathrm{a}}$) and strain of the graphene-PMMA membrane by the three actuation methods have been calculated. As the actuated tension changes with different actuation methods, the measured resonant frequencies vary.

TABLE II
OVERALL TENSION ($N_{\mathrm{i}} + N_{\mathrm{a}}$) AND STRAIN IN THE GRAPHENE-PMMA MEMBRANE DEDUCTED FROM THE MEASURED RESONANT FREQUENCY

Actuation methods	*Measured resonant frequency* (kHz)	*Tension* (N/m)	*Strain* (%)
Mechanical	11.72	2.09	0.057
Acoustic	10.58	1.74	0.046
Electro-thermal	10.01	1.53	0.041

TABLE III
POSITIONS AND FULL WIDTH AT HALF MAXIMUM (FWHM) OF THE G AND 2D PEAKS.

	G		2D	
	position (cm^{-1})	FWHM (cm^{-1})	position (cm^{-1})	FWHM (cm^{-1})
Center	1589.7	23.2	2693.4	39.24
Substrate	1592.5	27.01	2703.4	35.03

2) Raman spectroscopy: Raman spectroscopy measurement has been taken on the suspended membrane′s center and with the membrane on the substrate respectively, using 0.8 mW laser power, with laser excitation of 514.5 nm and a 100x objective. The experiment has been conducted on four different and random points around the suspended graphene-PMMA membrane's center and on the membrane stuck on the substrate respectively. The Raman spectrum observed from the selected points have been consistent. Fig. 8 shows the Raman spectrum of the graphene-PMMA closed cavity resonator. The dash lines represent plots of the Lorentz Fitting. Fig. 8(a) illustrates the appearance of the D peak, G peak, 2D peak and 2D′peak, which shows the graphene-PMMA membrane is suspended over the closed cavity when using the Kapton tape dry transfer method. The narrow shape of G peak and 2D peak indicates that the graphene film

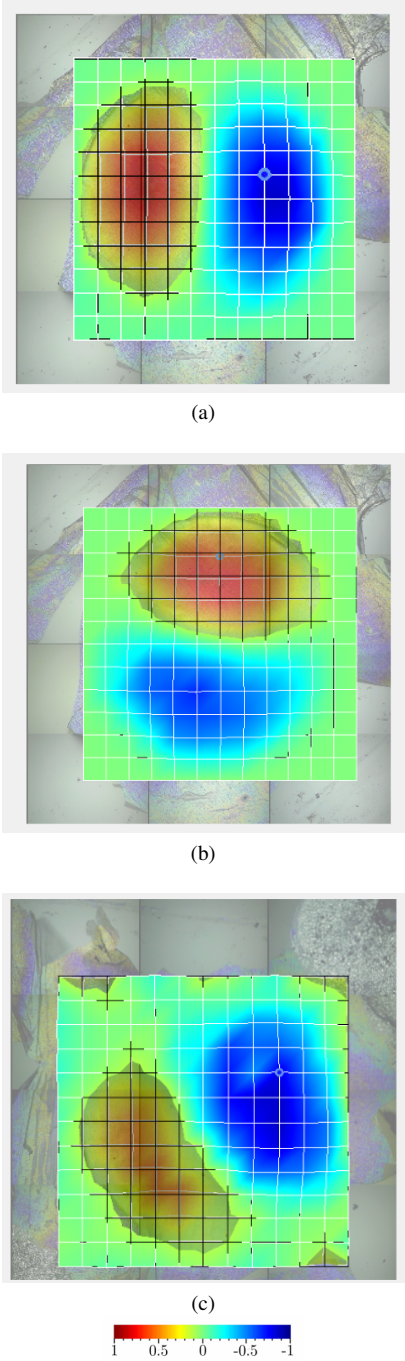

Fig. 6. The (1, 1) mode shape of the membrane over closed cavity substrate on resonant frequency actuated: (a) mechanically with 0.1 V AC; (b) by 40 dB sound pressure; (c) electro-thermally with 1 V AC and 1 V DC.

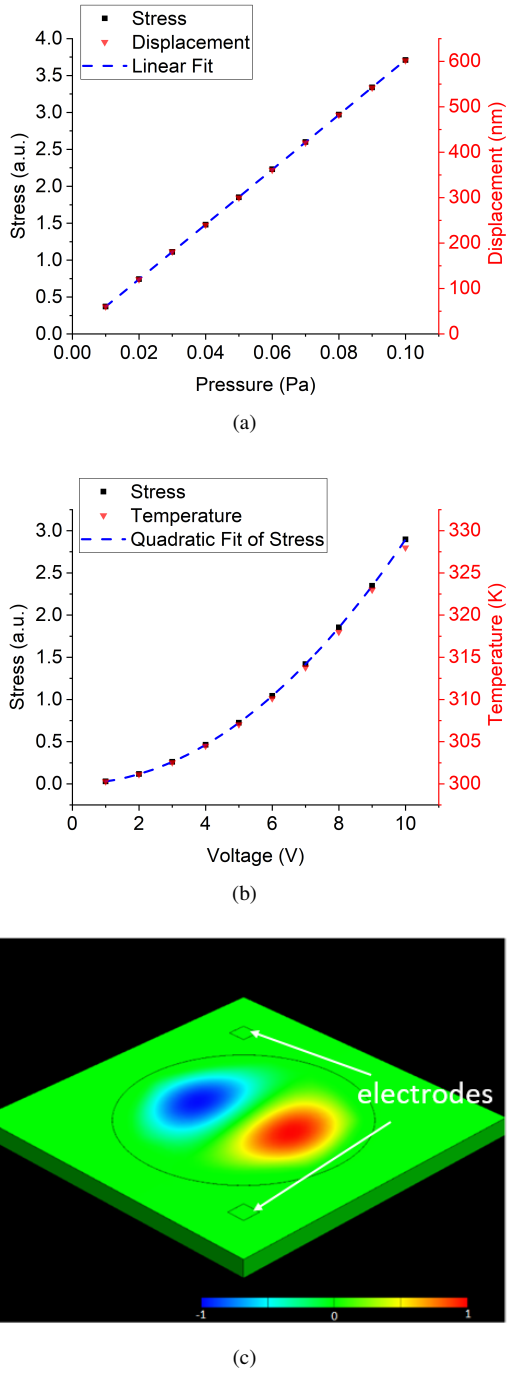

Fig. 7. FEA simulations: (a) Simulated stress (black square) and displacement (red triangle) of the membrane versus input pressure; (b) simulated thermal stress (black square) and temperature (red triangle) of the membrane with respect to input voltage; (c) simulated mode shape of the membrane under the mechanical and electro-thermal actuation.

is between 5 to 10 layers [22], which agrees with the fact that the graphene on copper foil is 6 layers before transfer. The intensity ratio between D peak and G peak has been estimated to be 0.51, which indicates, the graphene sample is defected [22]. However, from visual inspection, no large scale defects have been found. The appearance of D peak in the suspended structure of graphene might be due to structural disorder [23], [24]. Fig. 8(b) and Fig. 8(c) show the Raman shift of 2D peak and G peak between the graphene-PMMA membrane suspended over the closed cavity and stuck on the substrate. As Table III shows, compared to the membrane on the substrate, 2D peak and G peak of suspended membrane′s center have been detected to shift by 10.0 cm^{-1} and 2.8 cm^{-1}. The shift of the 2D peak and G peak positions related to biaxial tensile strain in graphene has been measured to be -77 ± 7 $cm^{-1}/\%$ and -203 ± 20 $cm^{-1}/\%$, in the previous work [25]. With the Raman shift, the strain of the suspended

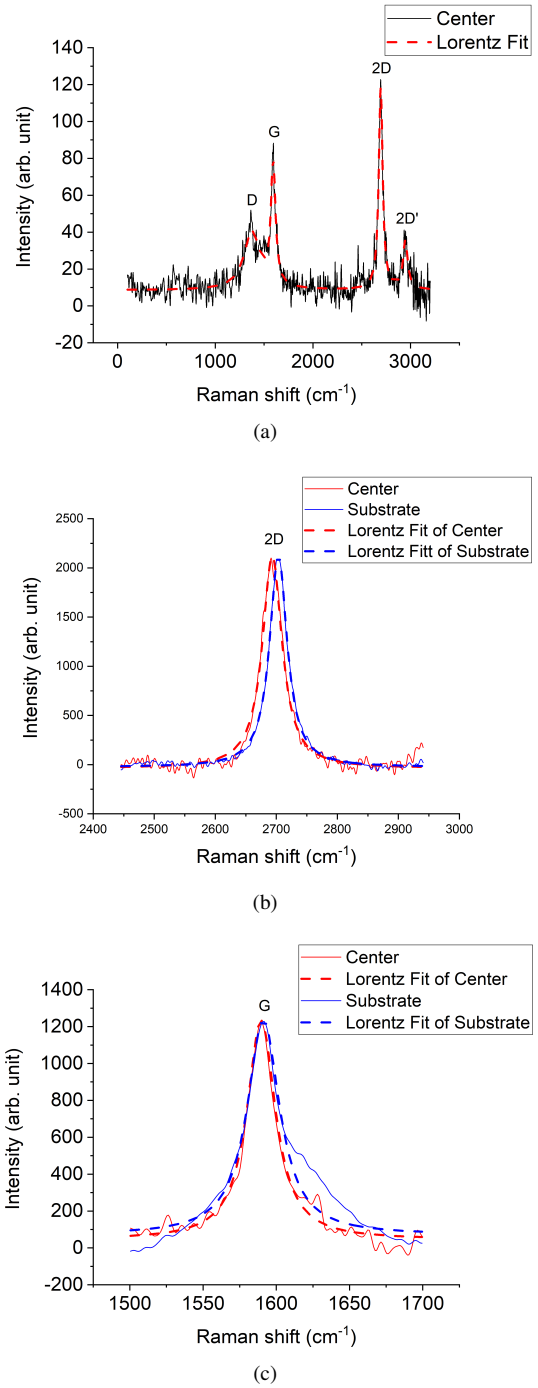

Fig. 8. The Raman spectrum of the graphene-PMMA closed cavity resonator: (a) full scan of the Raman spectrum at the center of the suspended membrane; (b) 2D peak position shift of suspended membrane′s center (red) and the membrane stuck on the substrate (blue); (c) G peak position shift of suspended membrane's center (red) and the membrane stuck on the substrate (blue).

graphene-PMMA membrane is estimated to be 0.04 $\pm 0.01\%$.

In the case of the electro-thermal actuation, the strain, which is deduced from the resonant frequency, in the graphene-PMMA membrane is the smallest amongst the three different actuation methods. The value of the strain in the graphene-PMMA membrane with electro-thermal actuation drops by about 24 % compared to other two actuation methods. The observation might be due to the strain softening generated by Joule Heating.

The bi-axial tensile strain estimated from the Raman shift is associated only with the built-in tension (N_{i}). The tensile strain deduced from resonant frequency is related to both the built-in tension (N_{i}) and actuation tension (N_{a}). The value of the strain in the membrane deduced from the measured resonant frequency and the one calculated from the Raman shift is similar, which suggests that the built-in tension dominates the overall in-plane tension in the three actuation methods. Therefore, the overall strain in the graphene based membrane suspended over the closed cavity, is estimated to be 0.04 $\pm 0.01\%$.

Finally, table IV shows a comparison of our work to other research on graphene-based acoustic sensors.

V. Conclusion

In summary, it is the first time that an ultra large area graphene-PMMA closed cavity resonator has been fabricated and actuated successfully. The ultra-large graphene-PMMA membrane has been dry transferred using Kapton tape as a supporting frame. The modified dry transfer method has been tested with about 95 % percentage yield over 20 samples. Raman spectrum confirms that the ultra large graphene membrane has been transferred safely using the modified graphene dry transfer method. The WLI results indicate that the dry transfer method can be used to transfer graphene-PMMA membrane over the large area closed cavity with small static deformation. The fact that (1, 1) mode resonant frequency dominates, suggests gas encapsulation is good in comparison to open cavity designs with the same suspended graphene-PMMA membrane size, in which the (0, 1) mode frequency is dominant. Furthermore, the frequency response of the graphene-PMMA membrane suspended on closed cavity resonator actuated mechanically, acoustically and electro-thermally, has been characterized in this work. In agreement with the experimental results, FEA simulations have shown that the membrane's displacement and stress during actuation vary linearly as a function of either the applied mechanical force or the applied acoustic pressure. Similarly, the quadratic relationship between the electro-thermal actuation voltage and the stress has been confirmed with FEA simulations. The overall strain in the graphene-PMMA membrane suspended over the closed cavity is estimated to be 0.04 $\pm 0.01\%$. The metric acoustic vibration amplitude sensitivity of the multilayer graphene-PMMA membrane over the closed cavity indicates the promise of achieving high quality graphene-PMMA microphones with high sensitivity.

References

[1] J. S. Bunch, A. M. Van Der Zande, S. S. Verbridge, I. W. Frank, D. M. Tanenbaum, J. M. Parpia, H. G. Craighead, and P. L. McEuen, "Electromechanical resonators from graphene sheets," *Science*, vol. 315, no. 5811, pp. 490–493, 2007.

[2] S. Lee, C. Chen, V. V. Deshpande, G.-H. Lee, I. Lee, M. Lekas, A. Gondarenko, Y.-J. Yu, K. Shepard, P. Kim *et al.*, "Electrically integrated su-8 clamped graphene drum resonators for strain engineering," *Applied Physics Letters*, vol. 102, no. 15, p. 153101, 2013.

TABLE IV
COMPARISON OF OUR WORK TO OTHER RESEARCH ON GRAPHENE-BASED ACOUSTIC SENSORS

	Graphene layers number	PMMA thickness	Overall membrane thickness	Aspect ratio	Fabrication process	Actuation method	Sensitivity	Resonant frequency
This work	6	450 nm	452 nm	7800	One step	Mechanical, acoustic and electro-thermal	**Mechanical**: 119.74 nm/V; **Acoustic**: 6.06 μm/Pa; **Electro-thermal**: 0.3 nm/V^2;	Around 10 k
[11]	75	0 nm	25 nm	350,000	With supporting frame and manual assemble method	Acoustic	-70 dBV	NA
[12]	1800	1 μm	1.2 μm	3400	With supporting frame and manual assemble method	Acoustic	-20 dBV	3.2K
Our work [13]	5	198 nm	200 nm	15,000	With supporting frame and manual assemble method	Acoustic	-40 dBV	NA
Our work [14]	8	370 nm	373 nm	9,400	Wet transfer on open cavity	Electro-thermal	3.4 nm/V	4k

[3] C. Wong, M. Annamalai, Z. Wang, and M. Palaniapan, "Characterization of nanomechanical graphene drum structures," *Journal of Micromechanics and Microengineering*, vol. 20, no. 11, p. 115029, 2010.

[4] P. Weber, J. Guttinger, I. Tsioutsios, D. E. Chang, and A. Bachtold, "Coupling graphene mechanical resonators to superconducting microwave cavities," *Nano letters*, vol. 14, no. 5, pp. 2854–2860, 2014.

[5] J. P. Mathew, R. N. Patel, A. Borah, R. Vijay, and M. M. Deshmukh, "Dynamical strong coupling and parametric amplification of mechanical modes of graphene drums," *Nature nanotechnology*, vol. 11, no. 9, p. 747, 2016.

[6] R. J. Dolleman, D. Davidovikj, S. J. Cartamil-Bueno, H. S. van der Zant, and P. G. Steeneken, "Graphene squeeze-film pressure sensors," *Nano letters*, vol. 16, no. 1, pp. 568–571, 2015.

[7] R. Singh, R. J. Nicholl, K. I. Bolotin, and S. Ghosh, "Motion transduction with thermo-mechanically squeezed graphene resonator modes," *Nano letters*, vol. 18, no. 11, pp. 6719–6724, 2018.

[8] K. I. Bolotin, K. Sikes, Z. Jiang, M. Klima, G. Fudenberg, J. Hone, P. Kim, and H. Stormer, "Ultrahigh electron mobility in suspended graphene," *Solid State Communications*, vol. 146, no. 9-10, pp. 351–355, 2008.

[9] A. Al-mashaal, G. Wood, A. Torin, E. Mastropaolo, M. Newton, and R. Cheung, "Dynamic behavior of ultra large graphene-based membranes using electrothermal transduction," *Applied Physics Letters*, vol. 111, no. 24, p. 243503, 2017.

[10] Q. Zhou, J. Zheng, S. Onishi, M. Crommie, and A. K. Zettl, "Graphene electrostatic microphone and ultrasonic radio," *Proceedings of the National Academy of Sciences*, vol. 112, no. 29, pp. 8942–8946, 2015.

[11] D. Todorović, A. Matković, M. Milićević, D. Jovanović, R. Gajić, I. Salom, and M. Spasenović, "Multilayer graphene condenser microphone," *2D Materials*, vol. 2, no. 4, p. 045013, 2015.

[12] S. Woo, J.-H. Han, J. H. Lee, S. Cho, K.-W. Seong, M. Choi, and J.-H. Cho, "Realization of a high sensitivity microphone for a hearing aid using a graphene–pmma laminated diaphragm," *ACS applied materials & interfaces*, vol. 9, no. 2, pp. 1237–1246, 2017.

[13] G. S. Wood, A. Torin, A. K. Al-mashaal, L. S. Smith, E. Mastropaolo, M. J. Newton, and R. Cheung, "Design and characterization of a microfabricated graphene-based mems microphone," *IEEE Sensors Journal*, 2019.

[14] A. K. Al-Mashaal, G. S. Wood, A. Torin, E. Mastropaolo, M. J. Newton, and R. Cheung, "Tunable graphene-polymer resonators for audio frequency sensing applications," *IEEE Sensors Journal*, vol. 19, no. 2, pp. 465–473, 2018.

[15] Q. Zhou and A. Zettl, "Electrostatic graphene loudspeaker," *Applied Physics Letters*, vol. 102, no. 22, p. 223109, 2013.

[16] K. Takahashi, H. Ishida, and K. Sawada, "Vacuum-sealed microcavity formed from suspended graphene by using a low-pressure dry-transfer technique," *Applied Physics Letters*, vol. 112, no. 4, p. 041901, 2018.

[17] J. W. Suk, A. Kitt, C. W. Magnuson, Y. Hao, S. Ahmed, J. An, A. K. Swan, B. B. Goldberg, and R. S. Ruoff, "Transfer of cvd-grown monolayer graphene onto arbitrary substrates," *ACS nano*, vol. 5, no. 9, pp. 6916–6924, 2011.

[18] L. Que, J.-S. Park, and Y. Gianchandani, "Bent-beam electro-thermal actuators for high force applications," in *Technical Digest. IEEE International MEMS 99 Conference. Twelfth IEEE International Conference on Micro Electro Mechanical Systems (Cat. No. 99CH36291)*. IEEE, 1999, pp. 31–36.

[19] N.-T. Nguyen, S.-S. Ho, and C. L.-N. Low, "A polymeric microgripper with integrated thermal actuators," *Journal of Micromechanics and Microengineering*, vol. 14, no. 7, p. 969, 2004.

[20] J. S. Bunch, S. S. Verbridge, J. S. Alden, A. M. Van Der Zande, J. M. Parpia, H. G. Craighead, and P. L. McEuen, "Impermeable atomic membranes from graphene sheets," *Nano letters*, vol. 8, no. 8, pp. 2458–2462, 2008.

[21] Y. Zhou and F. Amirouche, "Study of fluid damping effects on resonant frequency of an electromagnetically actuated valveless micropump," *The International Journal of Advanced Manufacturing Technology*, vol. 45, no. 11-12, p. 1187, 2009.

[22] A. C. Ferrari, J. Meyer, V. Scardaci, C. Casiraghi, M. Lazzeri, F. Mauri, S. Piscanec, D. Jiang, K. Novoselov, S. Roth *et al.*, "Raman spectrum of graphene and graphene layers," *Physical review letters*, vol. 97, no. 18, p. 187401, 2006.

[23] A. C. Ferrari, "Raman spectroscopy of graphene and graphite: disorder, electron–phonon coupling, doping and nonadiabatic effects," *Solid state communications*, vol. 143, no. 1-2, pp. 47–57, 2007.

[24] A. C. Ferrari and J. Robertson, "Interpretation of raman spectra of disordered and amorphous carbon," *Physical review B*, vol. 61, no. 20, p. 14095, 2000.

[25] C. Metzger, S. Rémi, M. Liu, S. V. Kusminskiy, A. H. Castro Neto, A. K. Swan, and B. B. Goldberg, "Biaxial strain in graphene adhered to shallow depressions," *Nano letters*, vol. 10, no. 1, pp. 6–10, 2009.